Ultrafast Dynamics of Chlorine−Water and Bromine−Water Radical Complexes Following Electron Photodetachment in Their Anionic Precursors

Martina Roeselová,[†] Uzi Kaldor,[‡] and Pavel Jungwirth*,[†]

J. Heyrovský Institute of Physical Chemistry, Academy of Sciences of the Czech Republic, Dolejskova 3, 18223 Prague 8, Czech Republic, and School of Chemistry, Tel Aviv University, 69978 Tel Aviv, Israel

Received: January 20, 2000; In Final Form: May 2, 2000

Picosecond dynamics initiated by electron photodetachment in $Cl^-\cdots H_2O$ and $Br^-\cdots H_2O$ complexes is explored using classical Wigner trajectories which correctly map the initial quantum vibrational state of the systems. The three lowest potential energy surfaces of the neutral clusters reached after electron photodetachment are constructed by the ab initio Fock-Space Coupled Cluster Method and then quantitatively fitted to a Diatomics-in-Molecule Model which also allows for a simple inclusion of spin−orbit interactions. Because of large differences between the shapes of the anionic and neutral potential energy surfaces, and due to the presence of light hydrogen atoms, an unusual dynamical behavior is observed. Although the vertical photodetachment process places the systems above the dissociation threshold, the clusters do not dissociate directly. Instead, relatively long-lived vibrational resonances are observed. This is due to a strong excitation of the nondissociative (internal) water rotation and only a weak excitation of the dissociative intermolecular stretch upon photodetachment. Implications of the observed dynamics for the interpretation of experimental vibrationally resolved ZEKE spectra are discussed.

I. Introduction

Considerable attention has been devoted recently to the elucidation of structure and energetics of size selected anionic halogen−water clusters. Studies of sequential solvation of halogen anions in water clusters contribute to our understanding of salt solvation in a polar medium at a detailed microscopic level. At the same time, interesting questions pertinent to the cluster environment arise. For example, it has been shown that unlike alkali cations halogen anions do not become fully solvated but rather occupy surface sites on small and medium-sized water clusters.[1] These clusters have been explored theoretically using methods of ab initio quantum chemistry,[2−4] molecular dynamics,[1,5−7] and Monte Carlo,[8] as well as experimentally, by means of photoelectron[9,10] and infrared[11,12] spectroscopies.

With the advent of the anion zero electron kinetic energy (ZEKE) spectroscopy,[13−16] scientific interest has encompassed also the corresponding neutral clusters, prepared by electron photodetachment. The reason is that ZEKE spectroscopy has reached a resolution of ~ 1 cm^{-1} (unheard of in conventional photoelectron spectroscopy), thus being able to probe intermolecular vibrational motions, primarily not in the anionic precursor, however, but rather in the nascent neutral cluster. Such vibrational motions have been studied, e.g., in size-selected halogen−argon clusters by means of classical and quantum molecular dynamics,[17−19] with the aim of reproducing and interpreting the experimental ZEKE spectra.[20,21] A $X^-\cdots Ar$ (X = Cl, Br, or I) cluster is structurally rather simple and the interpretation of the ZEKE signal in terms of excitation of the halogen−rare gas stretching motion by a vertical promotion to one of the three lowest neutral potential energy surfaces is relatively straightforward. This weak stretching excitation by the photodetachment process is due to a slight difference in optimal halogen-rare gas distances in the anionic and neutral complexes. The whole process is a bound-to-bound transition, and consequently, the clusters do not dissociate.

The halogen−water clusters are more complex and an unusual dynamical behavior upon electron photodetachment can be expected for two reasons. First, there is a major difference between the shapes of the anionic and neutral potential energy surfaces, not only in the intermolecular stretch but mainly in the angular coordinates.[22] While the anion has a nearly collinear X$^-$−H−O hydrogen bonded arrangement, in the neutral both hydrogens point away from the halogen atom. Second, there is a large mass ratio between the present heavy atoms and hydrogen. As a result of these two facts, the photodetachment process primarily leads to an excitation of the (internal) water rotation, as discussed further in this paper. This prevents direct fragmentation of the nascent neutral cluster into water and a halogen radical, although upon the loss of the excess electron the system is vertically promoted above the dissociation threshold.

In this study we investigate the ultrafast dynamics following electron photodetachment in $Br^-\cdots H_2O$ and $Cl^-\cdots H_2O$ clusters in direct connection with ZEKE experiments for these systems[23] and for the $I^-\cdots H_2O$ complex.[10] We first explore the three lowest neutral potential energy surfaces, corresponding to different orbital orientations of the unpaired *p*-electron of the halogen radical, by means of an accurate ab initio Fock-Space Coupled Cluster method[24,25] with a sufficiently flexible basis set. In the next step, we fit the ab initio points to a simple but quantitative Diatomics-in-Molecule model[26−28] which can be then used in dynamical calculations. Finally, on the picosecond time scale we generate a set of classical Wigner trajectories,[29,30] which correctly map the initial vibrational quantum state of the system. These trajectories are then analyzed and the main features of the dynamics on the lowest neutral surface are discussed.

[†] J. Heyrovský Institute of Physical Chemistry.
[‡] School of Chemistry.

10.1021/jp0002594 CCC: $19.00
Published on Web 06/24/2000

The paper is organized as follows. In the next section we describe the systems under study and the quantum chemical methods used for mapping the potential energy surfaces. The dynamical method is briefly described in section III, and in section IV the results are presented. Finally, the main findings are discussed and an outlook toward future work is presented in section V.

II. Systems and Potentials

A. Anionic Halogen−Water Clusters. In the present study, the anionic clusters represent precursors from which dynamics is initiated by electron photodetachment. For the purpose of constructing the initial wave packet (i.e., the harmonic vibrational ground-state wave function of the $X^-\cdots H_2O$ cluster), we have performed geometry optimization followed by vibrational analysis at the MP2/aug-cc-pVDZ and MP2/6-31++*g*** levels of theory for the $Cl^-\cdots H_2O$ and $Br^-\cdots H_2O$ complexes, respectively, using the Gaussian98 program.[31] The addition of diffuse functions is important for the correct description of the anion and the method and basis sets employed are similar to those proved recently to provide near-convergence in structural and energetic properties of $Cl^-\cdots H_2O$.[4]

B. Neutral Halogen−Water Clusters. Until recently, no reliable description of the three low-lying potential energy surfaces of the neutral $X^\bullet\cdots H_2O$ complexes arising from three different orientations of the singly occupied p-orbital of the halogen atom existed. In our previous work,[22,32] we have reported on a thorough ab initio scan of these surfaces followed by fitting the ab initio points to a semiempirical Diatomics-in-Molecule (DIM) model for the $Cl^\bullet\cdots H_2O$ complex. Here, we apply this method also to the $Br^\bullet\cdots H_2O$ complex.

1. Ab Initio Calculations. The method applied here to $Br^\bullet\cdots H_2O$ is similar to the $Cl^\bullet\cdots H_2O$ study reported previously.[22] Approximately 500 points on the potential surface were calculated by the Fock-space coupled cluster method (FSCC).[24,25] The method has produced accurate predictions for different atomic and molecular properties, including different states of the $Cl^\bullet\cdots H_2O$, $F^\bullet\cdots H_2O$, $Cl^\bullet\cdots NH_3$, and $F^\bullet\cdots NH_3$ complexes.[33−35] A detailed description of the method has been given elsewhere.[25] The level of theory employed is coupled cluster with single and double excitations (CCSD), which incorporates all single and double excitations from occupied to unoccupied orbitals, as well as all their products and powers, into the wave function. The Fock-Space method as implemented by us starts from a closed-shell state ($Br^-\cdots H_2O$ in the present case), called the reference state, and correlates it. We then proceed to states obtained from the reference by the detachment of an electron from a set of preselected occupied orbitals (the four highest occupied orbitals here). These are correlated in turn by the CCSD method.

The augmented correlation-consistent pVDZ basis set of Dunning and co-workers[36−40] is used. It includes 3s2p contracted Gaussian-type orbitals on H, 4s3p2d on O, and 6s5p3d on Br. This is comparable to or slightly better than bases used in our previous work,[22,33,34] and should give reliable potential surfaces.

2. Diatomics-in-Molecule Fit. The ab initio calculations at the FSCC level are highly accurate; however, they are computationally too demanding to allow for an extensive survey of the potential energy surface (PES) necessary for dynamical simulations. Therefore, an approximate but still reliable PES based on the ab initio points has to be constructed.

The specific feature of complexes involving an open-shell atom with a singly occupied *p*-orbital (P-atom) and one or more closed-shell species is given by the electronic structure of the open-shell atom that induces an anisotropy of the interaction. Because of this fact we cannot fit the ab initio data to a standard pairwise intermolecular potential. There is, however, a well-established semiempirical approach for treating the above problem for the case of an open-shell P-atom interacting with closed shell atoms in the spirit of the DIM method.[26−28] In our previous work concerning the $Cl^\bullet\cdots H_2O$ complex,[22,32] as well as here for $Br^\bullet\cdots H_2O$, we extend this approach to the open-shell P-atom−closed-shell molecule case.

The lowest adiabatic potentials corresponding to the interaction between a P-atom and a single closed-shell atom are commonly denoted as $V_\Sigma(r)$ and $V_\Pi(r)$,[26,27] where Σ and Π stand for $\Lambda = 0$ and $\Lambda = 1$, respectively. Here, Λ is the absolute value of the projection of the orbital electronic angular momentum **L** on the interatomic axis *r*. An alternative approach is to express the interaction in terms of an expansion in Legendre polynomials, from which only the first two terms contribute:[26,27]

$$V(r,\theta) = V_0(r) + V_2(r)P_2(\theta) \tag{1}$$

Here, *r* is the interatomic distance, $P_2(\cos\theta)$ is the second Legendre polynomial, and θ is an electronic coordinate defined as the angle between the "axis" of the singly occupied *p*-orbital and the interatomic axis *r*. The relationship between the two representations of the interaction is in this case simply[26,27]

$$V_\Sigma = V_0 + \frac{2}{5}V_2 \tag{2}$$

and

$$V_\Pi = V_0 - \frac{1}{5}V_2 \tag{3}$$

Note that V_0 represents the spherically averaged contribution to the interaction, while V_2 is responsible for the $\Sigma-\Pi$ splitting.

The interaction between an open-shell P-atom and more than one closed-shell atoms can be written formally as a sum of pairwise terms

$$V = \sum_{i=1}^{N} V^i \tag{4}$$

where *N* is the number of closed-shell atoms. However, each term V^i has the form given by eq 1 and contains an electronic degree of freedom (angle θ) defined above. Therefore, eq 4 does not constitute a potential in a Born−Oppenheimer sense, and in order to obtain adiabatic potential energy surfaces, it is necessary to diagonalize the total interaction *V* in an appropriate electronic basis.

In the case of the $X^\bullet\cdots H_2O$ clusters, we treat each of the X−O, $X-H_1$, and $X-H_2$ interactions separately using the DIM approach as in the case of an atomic solvent. This is certainly an approximation since the atoms forming the water molecule are not perfectly spherically symmetric. Nevertheless, as has been shown for $Cl^\bullet\cdots H_2O$ complex,[22,32] this approach is accurate enough to provide a near-quantitative fit to the ab initio points.

The total interaction between a halogen atom and a water molecule consists of electronic and spin−orbit contributions. Therefore, to obtain adiabatic PESs one has to diagonalize the total interaction in a basis corresponding to the electronic and spin states of the halogen atom. In our case, it is appropriate to represent the unpaired electron of the halogen atom in a space-fixed basis of the corresponding spherical harmonics multiplied by the spin functions $\{\psi_k\}_{k=1\ldots6} = (Y_{1,-1}\alpha, Y_{1,-1}\beta, Y_{1,0}\alpha, Y_{1,0}\beta, Y_{1,1}\alpha, Y_{1,1}\beta\}$.[41,42]

The practical implementation of this scheme in the dynamical simulations of X•···H_2O clusters is then as follows: In each step of the propagation we calculate in the above given basis the matrix elements of the electronic interaction for each of the Cl−O, Cl−H_1, and Cl−H_2 pairs (denoted below by index i)

$$(\mathbf{V}^i)_{jk} = \langle \psi_j | V_0^i(r_i) + V_2^i(r_i) P_2(\cos\theta_i) | \psi_k \rangle \quad (5)$$

and sum the three matrices $\mathbf{V}^i$ into the resulting total electronic interaction matrix $\mathbf{V}$

$$\mathbf{V} = \sum_{i=1}^{3} \mathbf{V}^i \quad (6)$$

Then we add the matrix of the approximate spin−orbit operator[42]

$$\mathbf{H}_{SO} = \frac{2}{3}\Delta\, \mathbf{l}\cdot\mathbf{s} \quad (7)$$

where $\mathbf{l}$ is the orbital and $\mathbf{s}$ is the spin momentum operator of the unpaired electron, and Δ is the spin−orbit splitting between the $J = {}^3/_2$ and $J = {}^1/_2$ states of the halogen atom (equal to 0.102 eV for chlorine and to 0.457 eV for bromine[43]). This model assumes that there is negligible spin transfer from the halogen radical to the water molecule, which is generally very well satisfied in weakly bound intermolecular complexes.[42] Finally, the total 6×6 matrix is diagonalized, and the intramolecular potential energy of the water molecule[44] is added to the eigenvalues. The resulting energies correspond to the three doubly degenerate (Kramer's pairs) adiabatic energies of the cluster.

The $V_0(r)$ and $V_2(r)$ components of the X−H and X−O interactions have been obtained by fitting the first three low-lying ab initio potential energy surfaces of the neutral X•···H_2O complex for X = Cl and Br. For the isotropic X−O component V_0^O we use a Buckingham potential

$$V_0^O(r) = a_O \exp(-b_O r) - c_O/r^6 \quad (8)$$

while for the isotropic X−H component V_0^H a repulsive exponential potential

$$V_0^H(r) = a_H \exp(-b_H r) \quad (9)$$

is employed. The anisotropic component V_2 consists of two parts, the first part represents a correction to the spherically symmetric V_0 potential due to the asymmetry of the open-shell halogen atom,[26] while the second part corresponds to the interaction between the quadrupole moment Q of the halogen atom and the partial charges $q_H = 0.6e$ and $q_O = -1.2e$ of the hydrogen and oxygen atoms:[44,45]

$$V_2^O(r) = -A_O \exp(-B_O r) + C_O/r^6 + \frac{5}{2} q_O Q / r_d^3 \quad (10)$$

$$V_2^H(r) = -A_H \exp(-B_H r) + \frac{5}{2} q_H Q / r^3 \quad (11)$$

Here, r is the interatomic distance (i.e., X−O, X−H_1, or X−H_2 as appropriate) and r_d in eq 10 is the distance between the halogen and a dummy atom on which the negative partial charge of oxygen is placed.[44] The employment of this refined four-site model of water with the negative partial charge shifted slightly away from the oxygen atom leads to a substantially better agreement between the ab initio data and the fitted curves compared to the ordinary three-site model of water that we have originally used for the Cl•···H_2O complex.[22] The values of the halogen quadrupole moment $Q = 2.33$ DÅ for chlorine and $Q = 2.78$ DÅ for bromine have been calculated at the same level of theory as the cluster energies. In principle, terms corresponding to the polarization of the halogen by the water could also be added. However, their effect is relatively minor and we have obtained a satisfactory fit neglecting these terms.

Using the $V_0^O(r)$, $V_2^O(r)$, $V_0^H(r)$, and $V_2^H(r)$ model functions defined by eqs 8−11, we calculate for each given geometry of the X•···H_2O complex matrix elements of X−O, X−H_1, and X−H_2 interactions and sum them up (see eqs 5 and 6). Since we fit ab initio surfaces which do not contain the spin−orbit contribution, we use only the electronic basis $\{\psi_k\}_{k\,=\,1...3} = \{Y_{1,-1}, Y_{1,0}, Y_{1,1}\}$. Diagonalization of the resulting 3×3 matrix gives three eigenvalues, λ_1, λ_2, and λ_3. The total potential energies ϵ_1, ϵ_2, and ϵ_3 of the three states of the X•···H_2O complex are then calculated from the λ_1, λ_2, and λ_3 eigenvalues by adding the internal deformation energy of the water molecule E_{H_2O} in the given geometry[44] and an absolute term E_∞ representing the ab initio energy of the complex at infinitely large separation between the halogen atom and water molecule

$$\epsilon_k = \lambda_k + E_{H_2O} + E_\infty \; (k = 1, 2, 3) \quad (12)$$

Finally, the 10 parameters a_H, b_H, A_H, B_H, a_O, b_O, c_O, A_O, B_O, and C_O are optimized by fitting simultaneously all the three potential surfaces, i.e., by evaluating the differences between the calculated energies ϵ_1, ϵ_2, ϵ_3 and the corresponding ab initio energies E_1, E_2, E_3. The nonlinear fitting procedure minimizes the sum of squares of these differences by a standard Levenberg−Marquardt algorithm.[46]

In this way, a computationally simple procedure for calculating the potentials of the first three low-lying states of the X•···H_2O complexes using a single set of parameters for each halogen species is obtained. By employing an intermolecular water−water potential,[44,45] this procedure can readily be applied also to larger X•$(H_2O)_n$ clusters containing more than one water molecule.

III. Dynamical Method

Upon electron photodetachment in the X^-···H_2O complex, the ground state vibrational wave function is assumed to be vertically promoted to a neutral potential surface where it is no longer stationary and, therefore, evolves in time.

The dynamics of the neutral complex has been studied using the Wigner trajectories approach, i.e., by propagating a swarm of classical trajectories the initial coordinates and momenta of which have been generated by a Wigner mapping[29,30] of the initial wave packet. Thus, the quantum nature of the initial state of the system under study is accounted for in the propagation. The initial (anionic) vibrational ground state wave function has been constructed as a product of Gaussians corresponding to the six anionic normal modes (three intramolecular normal modes of the water molecule, intermolecular stretch, in-plane bend, and out-of-plane bend). The initial rotational state has been set to $J = 0$. A computationally moderately demanding number of 800 trajectories has proven to give converged results. All simulations were done in Cartesian coordinates using a standard Gear routine[47] with a time step of 0.07 fs. The (Hellmann−Feynman) forces have been evaluated analyticaly by explicitely differentiating the DIM Hamiltonian.

IV. Results

A. Anionic Clusters and Initial Conditions. From previous calculations,[2−4] as well as experimental studies,[11,12] it is known

TABLE 1: Ab Initio Optimized Geometries and Harmonic Frequencies of $Cl^-\cdots H_2O$ and $Br^-\cdots H_2O$ Complexes[a]

	$Cl^-\cdots H_2O$ (MP2/aug-cc-pVDZ)	$Br^-\cdots H_2O$ (MP2/6-31++g**)
$R(O-H_1)$	0.965	0.9633
$R(O-H_2)$	0.9922	0.9814
$R(O-X)$	3.136	3.3678
$\alpha(H_1-O-H_2)$	100.41	101.50
$\alpha(X-O-H_2)$	8.26	12.38
$\beta(O-X-H_1-H_2)$	180.0	180.0
ν_1	187	146
ν_2	354	299
ν_3	729	695
ν_4	1666	1675
ν_5	3372	3598
ν_6	3884	3944

[a] Interatomic distances in angströms, angles in degrees, and frequencies in cm^{-1}. H_2 is the hydrogen bonded and H_1 the dangling hydrogen.

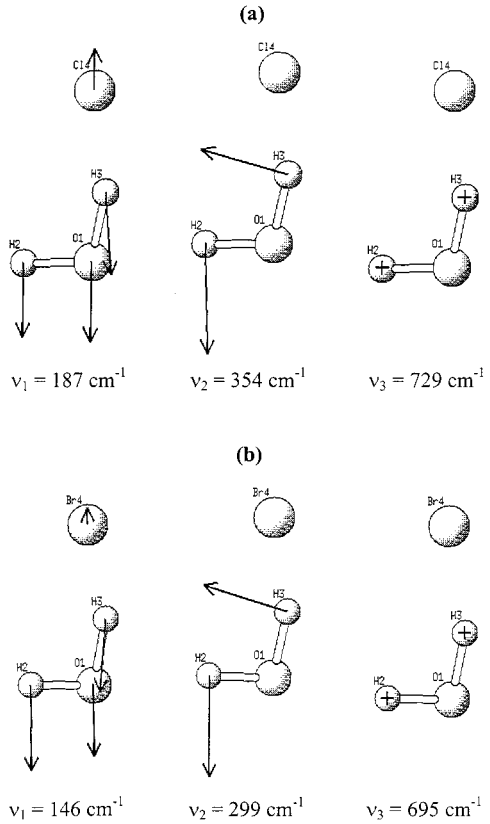

Figure 1. Optimal geometries and the three intermolecular normal mode vectors (ν_1 = halogen−water stretch, ν_2 = in-plane bend, ν_3 = out-of-plane bend) of (a) $Cl^-\cdots H_2O$ and (b) $Br^-\cdots H_2O$ complexes.

that the anionic halogen−water clusters $X^-\cdots H_2O$ have a planar geometry with a nearly collinear X^-−O−H arrangement. This hydrogen bonded structure is determined by the dipole−charge interaction between the strongly polar water molecule and the negatively charged halogen ion, as well as by the polarization interaction.

For the purpose of constructing the initial harmonic ground-state vibrational wave function of $X^-\cdots H_2O$ clusters, we have performed geometry optimizations followed by vibrational analysis at the MP2/aug-cc-pVDZ and MP2/6-31++g** levels of theory for $Cl^-\cdots H_2O$ and $Br^-\cdots H_2O$, respectively. The optimal geometrical parameters and harmonic vibrational frequencies of these two complexes are listed in Table 1, and the corresponding structures together with the three intermolecular normal mode vectors (halogen−water stretch, in-plane bend, and out-of-plane bend) are shown in Figure 1.

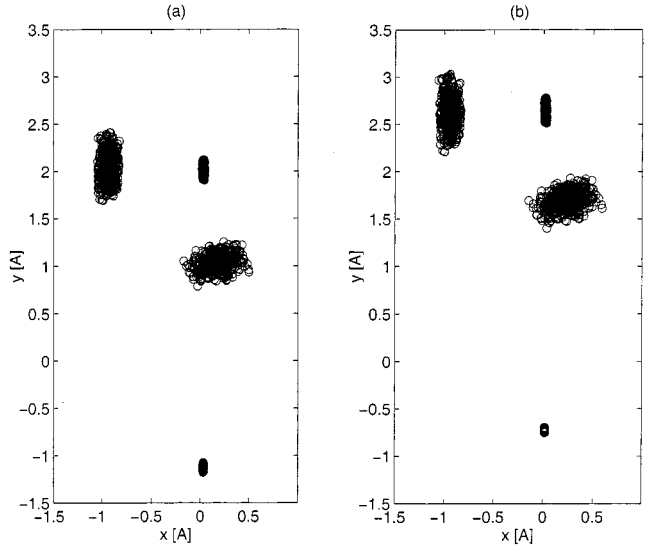

Figure 2. Delocalization of the atoms due to zero-point vibrations of (a) $Cl^-\cdots H_2O$ and (b) $Br^-\cdots H_2O$ complexes: initial conditions for a set of 800 Wigner trajectories.

TABLE 2: Optimal Values of Fitting Parameters for the Three Low-Lying Potential Energy Surfaces of $Cl^\bullet\cdots H_2O$ and $Br^\bullet\cdots H_2O$ Complexes

	$Cl^\bullet\cdots H_2O$	$Br^\bullet\cdots H_2O$
a_H (kcal mol^{-1})	5.92×10^2	2.22×10^3
b_H (Å^{-1})	2.40	2.88
A_H (kcal mol^{-1})	1.16×10^3	1.01×10^4
B_H (Å^{-1})	2.79	3.48
a_O (kcal mol^{-1})	7.76×10^4	7.70×10^4
b_O (Å^{-1})	3.29	3.20
c_O (kcal mol^{-1} Å^6)	3.40×10^3	3.59×10^3
A_O (kcal mol^{-1})	5.23×10^4	2.09×10^4
B_O (Å^{-1})	3.07	2.60
C_O (kcal mol^{-1} Å^6)	1.70×10^3	2.94×10^3

Using the $X^-\cdots H_2O$ harmonic frequencies and normal modes, the initial wave packet has been constructed as a product of the corresponding Gaussians. The initial conditions of the classical trajectories have been then obtained by mapping the initial wave function onto a weighted set of initial coordinates and momenta using the Wigner transformation.[29,30] As an illustration, the initial coordinate distribution for 800 trajectories showing the uncertainty in the positions of the atoms due to the $X^-\cdots H_2O$ ground state zero-point vibrations is depicted in Figure 2. Because of their small mass, the two hydrogens exhibit the largest spatial delocalization both for the in-plane and (especially the bound hydrogen) also for the out-of-plane motion, which is essential for the subsequent dynamics.

B. Neutral Potentials. The potential parameters obtained by fitting the first three low-lying ab initio surfaces of the $Cl^\bullet\cdots H_2O$ and $Br^\bullet\cdots H_2O$ complexes to the DIM potential model are listed in Table 2. The mean difference between the ab initio points and the fit is 0.4 kcal/mol in the full range of the fitted data, which is comparable to the accuracy of the ab initio calculation itself, and all the fitting parameters acquire physically meaningful values. Note that due to the employment of the four-site model of water in the DIM model the parameters for the $Cl^\bullet\cdots H_2O$ complex represent a refinement compared to our previously published results.[22]

Because of an analogous valence electronic structure of chlorine and bromine atoms, the three low-lying potential energy surfaces of $Cl^\bullet\cdots H_2O$ and $Br^\bullet\cdots H_2O$ complex have a rather similar character. As an illustration of the results of both the ab initio calculations and the quality of the fit, two different one-

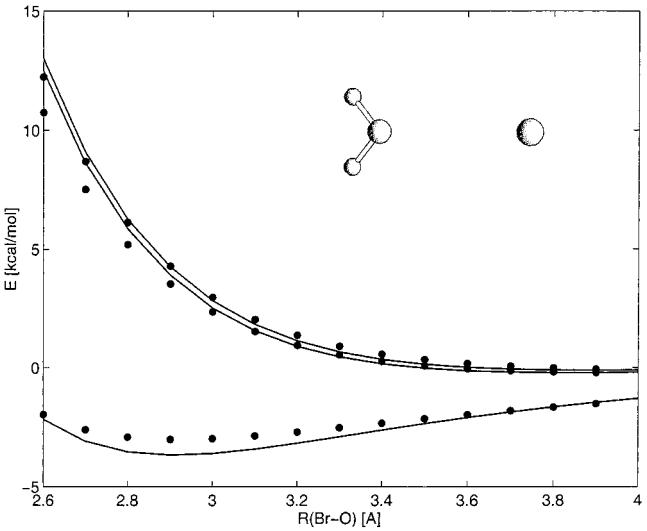

Figure 3. Potential energy curves of the first three low-lying states of the Br•···H_2O complex as a function of the Br−O distance for planar C_{2v} geometries with the two hydrogens pointing away from the Br atom. The dots correspond to ab initio points, full lines represent the DIM fit.

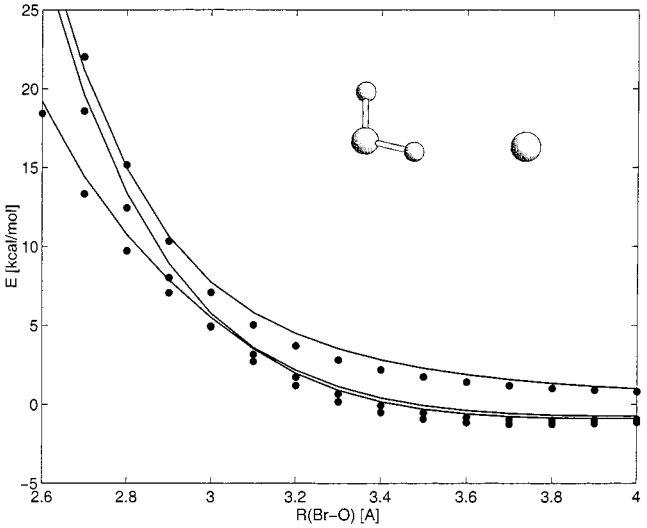

Figure 4. Potential energy curves of the first three low-lying states of the Br•···H_2O complex as a function of the Br−O distance for planar geometries with an asymmetric orientation of the H_2O molecule with respect to the Br atom close to the equilibrium (hydrogen-bonded) structure of the anionic Br^-···H_2O complex. The dots correspond to ab initio points, full lines represent the DIM fit.

dimensional cuts through the three surfaces of the Br•···H_2O complex are presented in Figures 3 and 4. In both cases, the potential energy curves have been obtained by varying the Br−O distance between 2.6 and 4.0 Å, while all the other geometrical parameters have been kept frozen. Figure 3 shows the three potential energy curves for planar geometries, the orientation of the H_2O molecule with respect to the Br atom being close to that for the global minimum of the Br•···H_2O complex (both hydrogens pointing away from the halogen atom). The lowest potential curve has a shape characteristic for a weakly bound state while the two upper states are almost purely repulsive. In Figure 4, the three potential energy curves are shown for a set of planar geometries with an asymmetric orientation of the water molecule, close to the equilibrium (hydrogen-bonded) structure of the anionic Br^-···H_2O complex. For the neutral Br•···H_2O complex, geometries of this kind are energetically rather unfavorable, which is clearly seen from the shapes of the potential energy curves depicted in Figure 4. The two lower states have only a very shallow minimum while the highest state is purely repulsive. Two states of the complex in planar geometries presented in Figure 4 are of the same A′ symmetry and exhibit an avoided crossing in the region of Br−O distances around 3 Å.

Generally, for both Cl•···H_2O and Br•···H_2O the DIM fit reproduces very well the overall shape of all three ab initio potential energy surfaces including avoided or true crossings of the potential curves, as well as the splittings between the three states. The largest deviations of the fitted curves from the ab initio points occur at short halogen−water separations; however, in the Franck−Condon region (around $R_{Cl-O} = 3.14$ Å or $R_{Br-O} = 3.36$ Å) as well as at large halogen−water separations, i.e., in those parts of the potential energy surfaces that are relevant for the dynamics, the agreement between the ab initio and fitted curves is quantitative.

As far as the ground-state minimum of the neutral X•···H_2O complexes is concerned, the DIM fit reproduces very well the depth (within 0.14 kcal/mol) and position (O−X distance within 0.1 Å) of the minimum. A minor problem is connected with the orientation of the water molecule with respect to the halogen atom, as discussed in detail in our previous work.[22] While the optimal geometry of the X•···H_2O complex obtained by the ab initio method is nonplanar (the X−O−H_1−H_2 dihedral angle of 105°), the DIM model prefers a planar structure with the hydrogens pointing away from the halogen atom (i.e., the X−O−H_1−H_2 dihedral angle equal to 180°). For this type of geometries the DIM fit slightly overestimates the bound character of the ground state and, at the same time, the repulsive character of the two upper states. The difference between the ab initio and DIM geometries of the ground state minimum is not negligible, the potential energy surface is, however, extremely flat with respect to the dihedral angle variation between 90° and 180°, and the system is very floppy here. Therefore, one particular geometry in this region is rather insignificant. Instead, it is important to reproduce the "plateau" region on the potential surface, which the DIM fit does reasonably well.

Theoretical calculations predict a significant difference between the equilibrium structures of the anionic and neutral complexes. In contrast to the hydrogen-bonded anionic X^-···H_2O structure, the ground state of the neutral X•···H_2O cluster has a minimum with both hydrogens pointing away from the halogen atom and a somewhat shorter X−O distance ($R_{Cl-O} = 2.7$ Å and $R_{Br-O} = 2.8$ Å). Such an optimal geometry can be rationalized in terms of the (halogen) quadrupole−(oxygen and hydrogens) partial charges interaction (see eqs 10 and 11) which represents the dominant contribution to the halogen−water intermolecular potential in the neutral system. As a result, the neutral clusters are less strongly bound, compared to their anionic counterparts.

The importance of the inclusion of the spin−orbit coupling term is demonstrated in Figures 5 and 6 on two-dimensional cuts through the potential energy surfaces of Cl•···H_2O and Br•···H_2O complexes. The pictures correspond to the region of the X−O distances between 2.5 and 4.0 Å and the full range (−180°, 180°) of the out-of-plane angle α between the interatomic X−O axis and the plane of the water molecule. The remaining intermolecular degree of freedom, i.e., the angle defining the in-plane orientation of the water molecule with respect to the halogen atom, has been fixed to the value corresponding to the optimized geometry of the anionic complex. We can see that the position and the depth of the

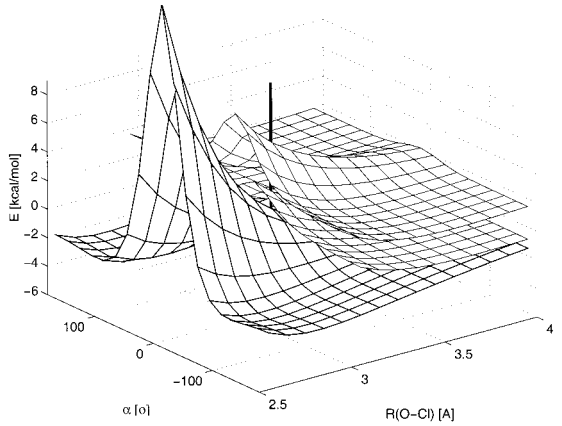

Figure 5. The first three low-lying potential energy surfaces (including the spin−orbit term) of the $Cl^{\bullet}\cdots H_2O$ complex as a function of the Cl−O distance and the out-of-plane angle α between the interatomic Cl−O axis and the plane of the water molecule. The H_2−O−Cl angle has been fixed to 8.26°. The vertical line intersects the three surfaces at the optimal geometry of the anion.

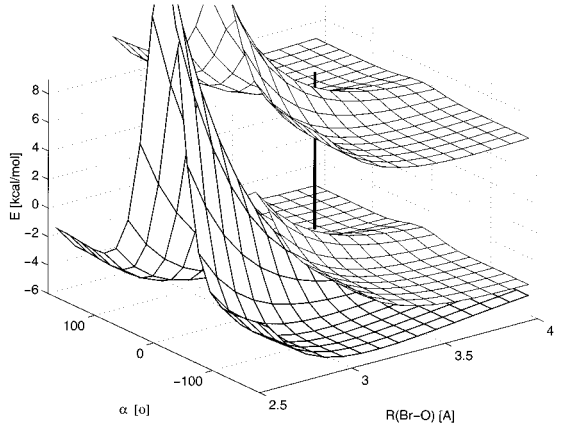

Figure 6. The first three low-lying potential energy surfaces (including the spin−orbit term) of the $Br^{\bullet}\cdots H_2O$ complex as a function of the Br−O distance and the out-of-plane angle α between the interatomic Br−O axis and the plane of the water molecule. The H_2−O−Br angle has been fixed to 12.38°. The vertical line intersects the three surfaces at the optimal geometry of the anion.

ground state minimum is practically unaffected by the spin−orbit interaction; however, the shapes of the surfaces in the region of dissociation of the complex are strongly influenced. The inclusion of the spin−orbit term lowers the dissociation threshold of the ground and first excited states by one-third of the spin−orbit constant Δ, thus enhancing the repulsive character of the latter. Simultaneously, the dissociation threshold of the second excited state increases by $^2/_3\Delta$, which makes this state more bound. In summary, the inclusion of the spin−orbit term is crucial for the quality of dynamical simulations.

C. Dynamics. Using the Wigner trajectories approach, we have studied the ultrafast dynamics following electron photodetachment in the anionic $Cl^-\cdots H_2O$ and $Br^-\cdots H_2O$ complexes. These simulations probe motions on the ground-state potential surface of the neutral $Cl^{\bullet}\cdots H_2O$ and $Br^{\bullet}\cdots H_2O$ clusters. In a forthcoming study we will explore also the dynamics on the first two excited surfaces. Since the three low-lying adiabatic neutral surfaces exhibit avoided crossings for certain geometries, possible nonadiabatic effects should also be investigated. Although we do not expect these effects to alter the present results qualitatively, we plan to simulate the electronically coupled problem both using surface hopping and by a rigorous quantum dynamical treatment.

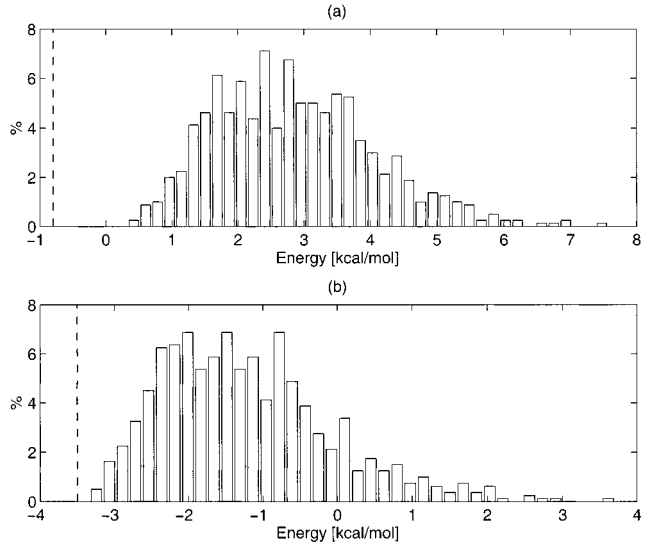

Figure 7. Distribution of the total energies for a set of 800 trajectories for (a) $Cl^{\bullet}\cdots H_2O$ and (b) $Br^{\bullet}\cdots H_2O$ complexes. The dashed line represents the ground-state dissociation threshold.

The anionic and neutral potentials differ significantly from each other, which results, e.g., in the aforementioned difference between the corresponding minima. A vertical transition of the initial (anionic) wave function onto the neutral ground-state surface initiated by the electron photodetachment process places the neutral system above the dissociation threshold (see Figures 5 and 6). This is demonstrated also in Figure 7, where the distribution of the total energies for 800 Wigner trajectories is depicted. As can be seen from Figure 7, the $Cl^{\bullet}\cdots H_2O$ complex has on average slightly more excess energy than the $Br^{\bullet}\cdots H_2O$ cluster, the latter being excited just above the dissociation limit.

Upon a vertical transition onto the neutral surface the initial vibrational wave packet is placed at and around the "ridge" corresponding to the planar (anion-like) geometries, far from the neutral ground-state minimum (see Figures 5 and 6). Moreover, the system has enough excess energy to dissociate directly. In classical simulations started from the above-described initial states, however, direct dissociation (within few tens of femtoseconds) of the $X^{\bullet}\cdots H_2O$ complex is observed only for a small fraction of trajectories. Although the (eventually dissociative) halogen−water stretching mode is excited, the large difference in the water orientation between the anionic and neutral minimum, as well as the fact that the hydrogens due to their small mass can readily respond to the initial forces, result primarily in the excitation of the (internal) rotation of the water molecule. Thus, most of the excess energy is at first deposited into the fast (nondissociative) rotational motion of the water molecule, which gives rise to a resonant state with a relatively long lifetime of several picoseconds (see Figure 11). On the picosecond time scale, the coupling between the angular and radial degrees of freedom leads to an energy transfer from the internal rotation of the water molecule to the halogen−water vibration, due to which the complex eventually dissociates for all trajectories.

As an illustration of the results of the dynamical simulations, the time evolution of the Cl−O and Br−O distances for the first 7 ps after electron detachment for representative sets of 10 trajectories is shown in Figures 8 and 9. Direct dissociation of the complex is represented by only a small fraction of trajectories. In most cases, however, the system remains bound for a certain period of time, long enough to perform one, several, or even many vibrations in the intermolecular halogen−water

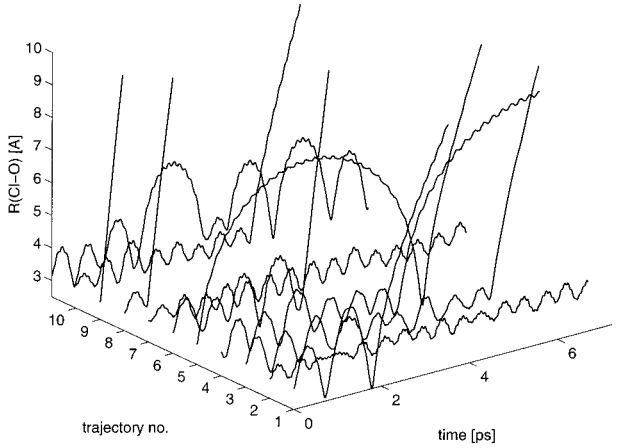

Figure 8. Time evolution of the Cl−O distance for a representative sets of 10 trajectories illustrating the early dynamics of the neutral Cl•···H_2O cluster.

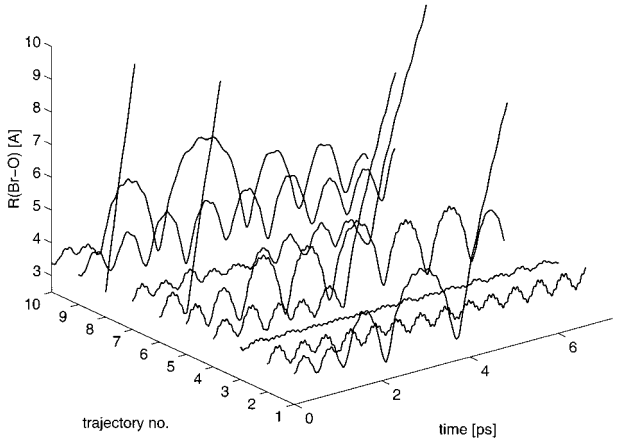

Figure 9. Time evolution of the Br−O distance for a representative sets of 10 trajectories illustrating the early dynamics of the neutral Br•···H_2O cluster.

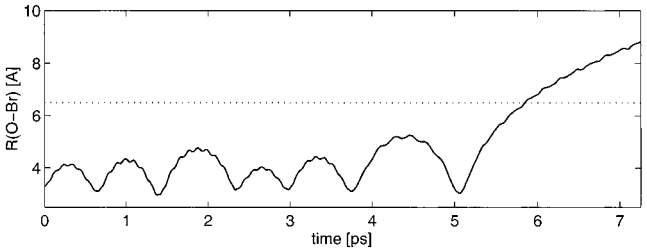

Figure 10. Time evolution of the Br−O distance for a typical quasi-bound trajectory. The dotted line at R(Br−O) = 6.5 Å represents the upper limit of the amplitude of the halogen−water vibration.

stretching mode, while at the same time, the water molecule is rotating fast. The dissociation behavior of the complex is strongly influenced by the anisotropy of the halogen−water potential both at the very beginning via the initial coordinate distribution as well as in the course of the dynamics through the coupling between the angular and radial degrees of freedom. Careful comparison of Figures 8 and 9 reveals also a quantitative difference between the dynamics of the Cl•···H_2O and Br•···H_2O complexes. As discussed below, the former cluster dissociates faster than the latter, which is mainly due to the different amount of the excess energy each of the systems acquires by the electron detachment process.

An example of a quasi-bound trajectory is presented in Figure 10, where again the Br−O distance is plotted against time (the results for the chlorine−water complex are very similar). The

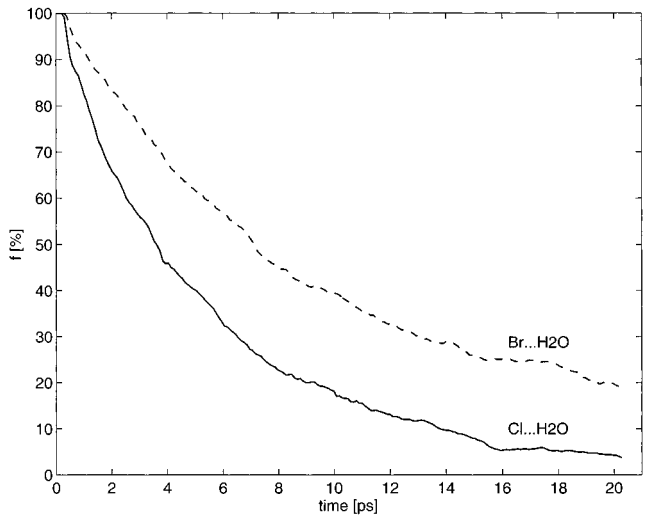

Figure 11. Fraction of undissociated Cl•···H_2O (full line) and Br•···H_2O (dashed line) complexes as a function of time for 800 trajectories.

large amplitude oscillations correspond to the halogen−water vibration, while the small oscillations are due to the fast rotation of the water molecule around its center of mass, in the course of which the distance of the two heavy atoms also slightly varies. The separation of time scales of the two motions is clearly seen here, while the intermolecular stretching mode has a period of roughly 700 fs, the internal water rotation is about seven times faster.

The comparison of the dissociative behavior of the Cl•···H_2O and Br•···H_2O complexes upon electron detachment is shown in Figure 11, where the fraction of undissociated complexes is plotted against time. For each individual trajectory (out of the total number of 800) the complex has been considered bound for distances between the two heavy atoms below 6.5 Å (an upper limit of the amplitude of the halogen−water vibration). The difference between the two complexes studied in this work can be quantified by fitting each of the two decay curves given in Figure 11 to an exponential function $y = Ae^{-kt}$ and by evaluating the corresponding lifetime $\tau = 1/k$. Using this procedure, average lifetimes $\tau_{Cl} = 5.8$ ps and $\tau_{Br} = 11.2$ ps have been obtained for the Cl•···H_2O and Br•···H_2O clusters, respectively.

V. Discussion and Conclusions

Three low-lying electronic surfaces of neutral X•···H_2O (X = Cl and Br) complexes have been described using an accurate ab initio Fock−space coupled cluster method and quantitatively fitted to a diatomics-in-molecule model, which also allows for a simple inclusion of the spin−orbit interaction. Using this fit, ultrafast dynamics following electron photodetachment in Cl^-···H_2O and Br^-···H_2O clusters has been explored by a large set of Wigner trajectories, the initial conditions of which faithfully map the quantum vibrational state of the anionic precursor.

For both clusters, the optimal anionic and neutral geometries differ significantly from each other. While the anion prefers a nearly collinear hydrogen-bonded X^-−H−O arrangement, the dominant quadrupole−quadrupole and dipole−quadrupole interactions in the neutral system orient both hydrogens away from the halogen atom reducing, at the same time, the X−O distance. The two halogen atoms differ primarily in the spin−orbit term, which is more than four times stronger for bromine than for

chlorine. As a results of these differences, upon vertical photodetachment the system is placed significantly (for chlorine) or slightly (for bromine) above the neutral ground state dissociation threshold. However, only about 10% of the Wigner trajectories are directly dissociative toward water and the halogen radical. The large heavy atom/hydrogen mass ratio together with the differences between the shapes of the anionic and neutral potential energy surfaces in the Franck−Condon region lead to a strong torque and consequently large (internal) rotational excitation of the water molecule. On the other hand, only a small fraction of the available energy is initially deposited in the dissociative coordinate, the halogen−water intermolecular stretch with a relatively large reduced mass. Note, however, that in order to correctly describe the rotational excitation of the water molecule one has to take into account the quantum delocalization of the initial vibrational wave packet, e.g., by employing Wigner trajectories. Neglecting this delocalization by initiating the dynamics following electron photodetachment from the optimal planar anionic geometry would lead to an exactly zero out-of-plane rotational excitation of the water molecule, since this geometry corresponds to an edge on the neutral PES with a vanishing torque.

The dynamics described above leads to unusual observable effects. First, although the excess energy after photodetachment is not small, the clusters on average perform several intermolecular stretching vibrations before dissociation. Therefore, resonances with a relatively long lifetime of 6 ps for chlorine and 11 ps for bromine should be observed. Second, the photodetachment process results in a much stronger excitation of the (internal) water rotation than of the intermolecular stretch. Consequently, an inverse vibrational/rotational separation should occur in the spectrum, with a fine vibrational structure superimposed on each separate rotational line.

Vibrationally resolved spectra have been recorded for electron photodetachment from the $I^-\cdots H_2O$ complex using the ZEKE technique.[10] Currently, experiments are being performed also for the clusters investigated here.[23] At the same time, we are working on replacing the Wigner trajectories by numerically exact quantum dynamical simulations of the ultrafast processes following electron photodetachment in the $Cl^-\cdots H_2O$ and $Br^-\cdots H_2O$ complexes, which will not change the results qualitatively; however, it will allow for a quantitative modeling of the intensities of the ZEKE signal. To facilitate direct comparison with experiment, we are planning to describe the initial vibrational state beyond the harmonic approximation, to include also the remaining two low-lying neutral surfaces into the dynamical model, and to extend our potential surfaces and dynamics studies to the $I^-\cdots H_2O$ cluster. Finally, work is in progress on clusters containing more than one water molecule, where several dissociation channels open and the dynamics becomes even more complex.

Acknowledgment. We are grateful to Ulrich Boesl and Franz Schlicht for stimulating discussions and for providing us their experimental results prior to publication. This project is supported by a Grant B1010925 from the Granting Agency of the Academy of Sciences of the Czech Republic (to P.J.). Research at Tel Aviv University was supported by the U.S.−Israel Binational Science Foundation and by the Israel Science Foundation.

References and Notes

(1) Perera, L.; Berkowitz, M. J. *J. Chem. Phys.* **1991**, *95*, 1954.
(2) Combariza, J. E.; Kestner, N. R.; Jortner, J. *Chem. Phys. Lett.* **1993**, *203*, 423.
(3) Combariza, J. E.; Kestner, N. R.; Jortner, J. *J. Chem. Phys.* **1993**, *100*, 2851.
(4) Xantheas, S. S. *J. Phys. Chem.* **1996**, *100*, 9703.
(5) Perera, L.; Berkowitz, M. L. *J. Chem. Phys.* **1992**, *96*, 8288.
(6) Perera, L.; Berkowitz, M. L. *J. Chem. Phys.* **1994**, *100*, 3085.
(7) Yeh, I. C.; Perera, L.; Berkowitz, M. L. *Chem. Phys. Lett.* **1997**, *264*, 423.
(8) Dorset, H. E.; Watts, R. O.; Xantheas, S. S. *J. Phys. Chem. A* **1999**, *103*, 3351.
(9) Markovich, G.; Giniger, R.; Levin, M.; Cheshnovsky, O. J. *Chem. Phys.* **1991**, *95*, 9416.
(10) Baessmann, C.; Boesl, U.; Yang, D.; Drechsler, G.; Schlag, E. W. *Int. J. Mass Spectrosc. Ion Proc.* **1996**, *159*, 153.
(11) Choi, J.-H.; Kuwata, K. T.; Cao, Y.-B.; Okomura, M. *J. Phys. Chem. A* **1998**, *102*, 503.
(12) Ayotte, P.; Weddle, G. H.; Johnson, M. A. *J. Chem. Phys.* **1999**, *110*, 7129.
(13) Muller-Detlefs, K.; Schlag, E. W. *Annu. Rev. Phys. Chem.* **1991**, *42*, 109.
(14) Waller, I. M.; Kitsopoulos, T. N.; Neumark, D. M. *J. Chem. Phys.* **1990**, *94*, 2240.
(15) Gantefor, G.; Cox, D. M.; Kaldor, A. *J. Chem. Phys.* **1990**, *94*, 854.
(16) Drechsler, G.; Baessmann, C.; Boesl, U.; Schlag, E. W. *J. Mol. Spectrosc.* **1995**, *348*, 337.
(17) Brewer, M. L.; Hulme, J. S.; Manopoulos, D. E. *J. Chem. Phys.* **1997**, *106*, 4832.
(18) Jungwirth, P.; Gerber, R. B. *J. Chem. Phys.* **1995**, *102*, 8855.
(19) Jungwirth, P.; Schmidt, B.; Moiseyev, N. *Chem. Phys. Lett.* **1997**, *280*, 177.
(20) Zhao, Y.; Yourshaw, I.; Reiser, G.; Arnold, C. C.; Neumark, D. M. *J. Chem. Phys.* **1994**, *101*, 6538.
(21) Yourshaw, I.; Zhao, Y.; Neumark, D. M. *J. Chem. Phys.* **1996**, *105*, 351.
(22) Roeselova, M.; Jacoby, G.; Kaldor, U.; Jungwirth, P. *Chem. Phys. Lett.* **1998**, *293*, 309.
(23) Boesl, U. Private communication.
(24) Lindgren, I.; Morrison, J. *Atomic Many Body Theory*; Springer: Berlin, 1982.
(25) Kaldor, U. *Theor. Chim. Acta* **1991**, *80*, 427.
(26) Aquilanti, V.; Liuti, G.; Pirani, F.; Vecchiocattivi, F. *J. Chem. Soc., Faraday Trans.* **1989**, *85*, 955.
(27) Becker, C. H.; Cassavecchia, P.; Lee, Y. T. *J. Chem. Phys.* **1979**, *70*, 5477.
(28) Ellison, F. O. *J. Am. Chem. Soc.* **1963**, *85*, 3540.
(29) Wigner, E. *Phys. Rev.* **1932**, *40*, 749.
(30) Hillery, M.; O'Connel, R. F.; Scully, M. O.; Wigner, E. *Phys. Rep.* **1984**, *106*, 121.
(31) Frisch, M. J.; Trucks, G. W.; Schlegel, H. B.; Scuseria, G. E.; Robb, M. A.; Cheeseman, J. R.; Zakrzewski, V. G.; Montgomery, J. A., Jr.; Stratmann, R. E.; Burant, J. C.; Dapprich, S.; Millam, J. M.; Daniels, A. D.; Kudin, K. N.; Strain, M. C.; Farkas, O.; Tomasi, J.; Barone, V.; Cossi, M.; Cammi, R.; Mennucci, B.; Pomelli, C.; Adamo, C.; Clifford, S.; Ochterski, J.; Petersson, G. A.; Ayala, P. Y.; Cui, Q.; Morokuma, K.; Malick, D. K.; Rabuck, A. D.; Raghavachari, K.; Foresman, J. B.; Cioslowski, J.; Ortiz, J. V.; Stefanov, B. B.; Liu, G.; Liashenko, A.; Piskorz, P.; Komaromi, I.; Gomperts, R.; Martin, R. L.; Fox, D. J.; Keith, T.; Al-Laham, M. A.; Peng, C. Y.; Nanayakkara, A.; Gonzalez, C.; Challacombe, M.; Gill, P. M. W.; Johnson, B. G.; Chen, W.; Wong, M. W.; Andres, J. L.; Head-Gordon, M.; Replogle, E. S.; Pople, J. A. *Gaussian98*; Gaussian, Inc.: Pittsburgh, PA, 1998.
(32) Jungwirth, P.; Roeselova, M.; Gerber, R. B. *J. Chem. Phys.* **1999**, *110*, 9833.
(33) Markovich, G.; Cheshnovsky, O.; Kaldor, U. *J. Chem. Phys.* **1993**, *99*, 6201.
(34) Kaldor, U. *Z. Phys. D* **1994**, *31*, 279.
(35) Kaldor, U. In *Applied Many-Body Methods in Spectroscopy and Atomic Structure*; Mukherjee, D., Ed.; Plenum: New York, 1992; p 213;
(36) Dunning, T. H., Jr. *J. Chem. Phys.* **1989**, *90*, 1007.
(37) Kendall, R. A.; Dunning, T. H., Jr.; Harrison, R. J. *J. Chem. Phys.* **1992**, *96*, 6796.
(38) Woon, D. E.; Dunning, T. H., Jr. *J. Chem. Phys.* **1994**, *100*, 2975.
(39) Wilson, A. K.; Woon, D. E.; Peterson, K. A.; Dunning, T. H., Jr. *J. Chem. Phys.* **1999**, *110*, 7667.
(40) Basis sets were obtained from the Extensible Computational Chemistry Environment Basis Set Database, developed and distributed by the Molecular Science Computing Facility, Environmental and Molecular Sciences Laboratory, Pacific Northwest Laboratory, P.O. Box 999, Richland, WA 99352 (http://www.emsl.pnl.gov).

(41) Krylov, A. I.; Gerber, R. B.; Coalson, R. D. *J. Chem. Phys.* **1996**, *105*, 4626.
(42) Vala, M.; Pellow, R. *J. Chem. Phys.* **1989**, *90*, 5612.
(43) Lindgren, I.; Morrison, J. *Atomic Energy Levels*; National Bureau of Standards: Washington, 1952.
(44) Coker, D. F.; Watts, R. O. *J. Phys. Chem.* **1987**, *91*, 2513.
(45) Reimers, J. R.; Watts, R. O.; Klein, M. L. *Chem. Phys.* **1982**, *64*, 95.
(46) Press, W. H.; Teukolsky, S. A.; Vetterling, W. T.; Flannery, B. P. *Numerical Recipes in Fortran*; Cambridge Press: New York, 1992.
(47) Allen, M. P.; Tildesley, D. J. *Computer Simulation of Liquids*; Clarendon: Oxford, 1987.